ISSN 1063-7834, Physics of the Solid State, 2014, Vol. 56, No. 2, pp. 347–352. © Pleiades Publishing, Ltd., 2014.
Original Russian Text © V.A. Pustovarov, A.N. Razumov, D.I. Vyprintsev, 2014, published in Fizika Tverdogo Tela, 2014, Vol. 56, No. 2, pp. 343–348.

OPTICAL PROPERTIES

Luminescence of $LaBr_3$: Ce,Hf Crystals under Photon Excitation in the Ultraviolet, Vacuum Ultraviolet, and X-Ray Ranges

V. A. Pustovarov[a, *], A. N. Razumov[a], and D. I. Vyprintsev[b]

[a] *Yeltsin Ural Federal University, ul. Mira 19, Yekaterinburg, 620002 Russia*

* *e-mail: vpustovarov@bk.ru*

[b] *Stark Ltd. Company, pr. Marksa 14, Obninsk, Kaluga oblast, 249034 Russia*

Received June 10, 2013

Abstract—This study has been carried out using synchrotron radiation, time-resolved luminescence ultraviolet and vacuum ultraviolet spectroscopy, optical absorption spectroscopy, and thermal activation spectroscopy. It has been found that, in scintillation spectrometric crystals $LaBr_3$: Ce,Hf characterized by a low hygroscopicity, along with Ce^{3+} centers in regular lattice sites, there are Ce^{3+} centers located in the vicinity of the defects of the crystal structure. It has also been found that the studied crystals exhibit photoluminescence (PL) of new point defects responsible for a broad band at wavelengths of 500–600 nm in the PL spectra. The minimum energy of interband transitions in $LaBr_3$ is estimated as $E_g \sim 6.2$ eV. The effect of multiplication of electronic excitations has been observed in the range of PL excitation energies higher than 13 eV (more than $2E_g$). Thermal activation studies have revealed channels of electronic excitation energy transfer to Ce^{3+} impurity centers.

DOI: 10.1134/S1063783414020267

1. INTRODUCTION

Crystals $LaBr_3$: Ce are modern scintillation materials for spectrometric detectors of photon radiation. The $LaBr_3$: Ce crystals manufactured by Saint-Gobain Corporation are characterized by the relatively high light yield (~60000 photon/MeV), relatively fast decay of scintillation pulses (16–25 ns), and high stability of the parameters over a wide temperature range. Owing to the high energy resolution and good radiation resistance, these crystals can be used in spectrometry and various medical applications [1–3]. The mechanism of the formation of scintillation pulses in these crystals has been studied in sufficient detail due to investigations of the luminescence under excitation of different types, as well as due to research in electronic excitation energy transfer to Ce^{3+} impurity centers [4–7]. At present, the main problem is to investigate the energy nonproportionality of the light yield in the gamma-ray spectral range and, especially, in the X-ray region of the spectrum [8, 9]. In [8], this dependence was studied using synchrotron radiation (SR) in the X-ray spectral range (1.4–100 keV). The $d \longrightarrow f$ photoluminescence (PL) of Ce^{3+} ions and self-trapped excitons (STEs) in $LaBr_3$: Ce under photon excitation in the ultraviolet (UV) and vacuum ultraviolet (VUV) ranges was investigated only in [4, 5]. For $LaBr_3$, the authors of these works gave approximate estimates for the energy of the fundamental absorption edge $E_{fa} = 5.2$ eV, the energy of the exciton states of 5.4 eV, and the minimum energy of interband transitions $E_g = 5.9$ eV at $T = 10$ K. In more recent works, this result, presented in [4, 5], was constantly cited, although, subsequently, such studies of $LaBr_3$ crystals in the VUV range have not been performed and the obtained result is clearly ambiguous. Therefore, investigation of the fundamental absorption edge of these crystals and PL under the UV/VUV photon excitation remains an important problem.

In our previous works [10, 11], we investigated the energy nonproportionality of the light yield of $LaBr_3$: Ce crystals in the extreme ultraviolet (XUV) range from 45 to 290 eV. In [12], we presented the first results of our investigations of $LaBr_3$: Ce under PL excitation in the VUV range. Since $LaBr_3$: Ce crystals are hygroscopic, a special technique for growing $LaBr_3$: Ce crystals doped with hafnium was developed in Russia and patented [13]. Such $LaBr_3$: Ce,Hf crystals with a low hygroscopicity are of clear interest for practical spectrometry. Therefore, the purpose of this work was to investigate luminescence of the low-hygroscopic $LaBr_3$: Ce,Hf crystals produced in Russia. The work was performed using low-temperature time-resolved UV–VUV spectroscopy, optical absorption spectroscopy, and thermal activation spectroscopy.

2. DETAILS OF THE EXPERIMENT

2.1. PL Excitation in the UV and VUV Spectral Ranges

The time-resolved and conventional time-integrated PL spectra in the range of 1.5–5.0 eV, the time-resolved PL excitation spectra in the range of 3.7–32.0 eV, and the PL decay kinetics were measured

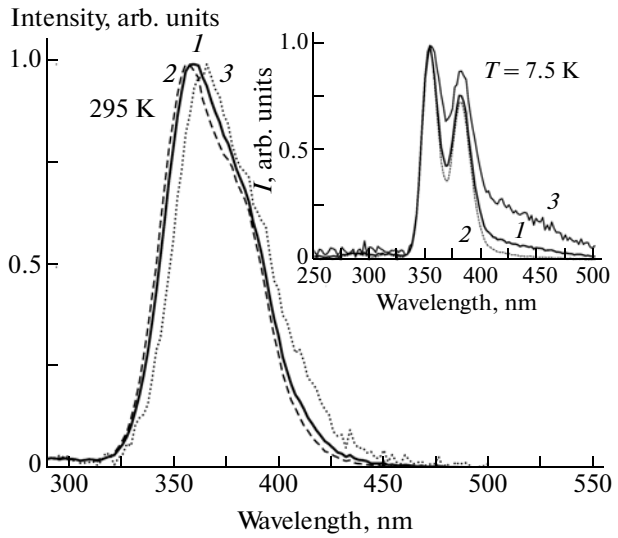

Fig. 1. Time-resolved PL spectra of $LaBr_3$: Ce at E_{exc} = 130 eV: (*1*) time-integrated, (*2*) fast, and (*3*) slow components. $T = 295$ K. The inset shows the PL spectra at $T = 7.5$ K.

using synchrotron radiation at the SUPERLUMI station (Hamburg Synchrotron Radiation Laboratory (HASYLAB) at the German Electron Synchrotron DESY, Hamburg, Germany). PL was excited using a monochromator with Al- or Pt-coated interchangeable gratings (the spectral resolution was 3.2 Å). The PL spectra were measured using a 0.3-m ARC Spectra Pro-308i monochromator and a Hamamatsu R6358P photomultiplier in two time windows $\Delta t_1 = 11$ ns (fast component) and $\Delta t_2 = 30$ ns (slow component), which were delayed relative to the start of the SR excitation pulse by $\delta t_1 = 3.0$ ns and $\delta t_2 = 36$ ns, respectively. The PL excitation spectra were normalized to equal numbers of photons incident on the sample with the use of sodium salicylate. The time resolution of the detection system was 0.8 ns (FWHM), and the time interval between SR pulses was 96 ns. Details of the experiment carried out under the XUV excitation can be found in [10, 11].

The PL excitation spectra in the low-energy range (2.8–5.5 eV) were measured using a 400 W deuterium discharge lamp and a DMR-4 double-prism monochromator. The PL excitation spectra were normalized to equal numbers of exciting photons using yellow phosphor.

2.2. X-Ray Luminescence and Thermal Activation Studies

The X-ray luminescence (XL) spectra and thermoluminescence (TL) curves were measured at the Ural Federal University using a URS-55A X-ray instrument (Cu anode, 30 kV, 10 mA), an MDR-23 monochromator, and a FEU-106 photomultiplier. The samples were irradiated at $T = 90$ K. The TL curves were measured at a constant heating rate of 0.3 K/s.

2.3. Samples

The studied single crystals of high optical quality (5 wt % cerium and 0.01–0.50 wt % hafnium in the charge) (Stark Ltd, Company, Obninsk, Russia) were grown by the Bridgman method in quartz ampoules at a rate of 1 mm/h [13]. The crystals were certified using X-ray diffraction, inductively coupled plasma mass spectrometry (ICP-MS), chemical and X-ray fluorescence analyses. According to the ICP-MS data, the content of the main impurities (Al, Ca, Zn, Ga) in the crystal was at a level of 10^{-3} wt %. The introduction of $HfBr_4$ into the initial melt, as shown in [13], decreases the hydroscopicity of the crystals. In this case, the Hf concentration in the studied crystals, according to the ICP-MS data, increases by two orders of magnitude, but, nonetheless, does not exceed 10^{-3} wt %.

A contact of hygroscopic $LaBr_3$ with the atmospheric air leads to a degradation of the sample surface due to the formation of crystal hydrates. Therefore, in our experiments, the studied samples ($5 \times 5 \times 1$ mm in size) were cleaved from the crystal boule in an atmosphere of a dry hot air and immediately mounted in a cryostat with a fast oil-free vacuum pumping (the residual working pressure in the cryostat was $\sim 1 \times 10^{-8}$ mbar).

3. EXPERIMENTAL RESULTS

The luminescence spectra of $LaBr_3$: Ce and $LaBr_3$: Ce,Hf under X-ray and XUV excitations are almost identical (Fig. 1). The spectra contain overlapping bands at 356 and 382 nm, which are formed by typical radiative $d \longrightarrow f$ transitions in the Ce^{3+} ion [1, 5, 6]. The XL efficiency of the Hf-doped crystals remains almost unchanged. An additional broad band with the maximum at 450 nm with the microsecond PL decay kinetics appears at low temperatures ($T <$ 100 K). According to [5], this band is formed by the STE radiation. The PL spectra depend substantially on the excitation energy E_{exc}. The PL spectrum of $LaBr_3$: Ce at $T = 8$ K under excitation by photons in the fundamental absorption region ($E_{exc} = 6.8$ eV) corresponds to the XL spectra or to the PL spectra under XUV excitation. On the contrary, the PL spectra of $LaBr_3$: Ce,Hf are shifted toward the long-wavelength range and contain narrow bands at 380 and 412 nm, as well as a broad band in the region of 500–600 nm with the microsecond PL decay kinetics (Fig. 2). A single-exponential decay kinetics is observed for the PL bands at 380 and 412 nm with the excitation energy $E_{exc} = 3.7$–5.0 eV and the decay time $\tau = 20 \pm 1$ ns. This decay time is shorter than the decay time of the Ce^{3+} luminescence in $LaBr_3$: Ce ($\tau = 23$–25 ns depending on the excitation energy E_{exc}; for more details, see [12]).

The PL excitation spectra for the 380 nm band at different temperatures and the absorption spectrum of $LaBr_3$: Ce,Hf (5%) are shown in Fig. 3. This figure

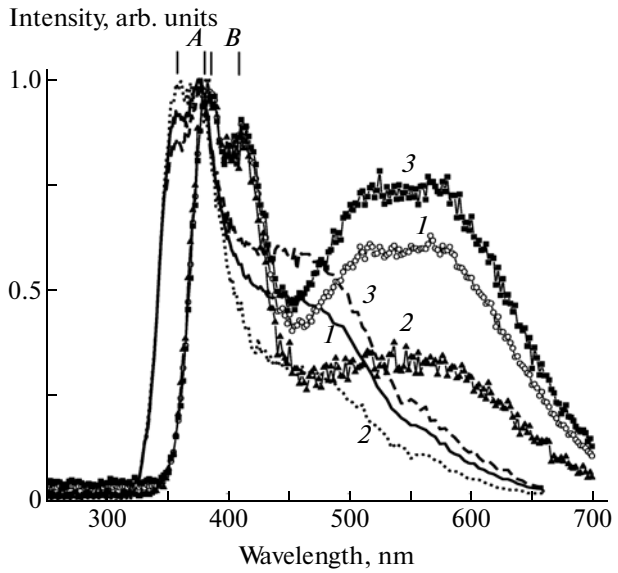

Fig. 2. Time-resolved PL spectra of $LaBr_3$: Ce (lines) and $LaBr_3$: Ce,Hf (points) at E_{exc} = 6.8 eV: (*1*) time-integrated, (*2*) fast, and (*3*) slow components. T = 8 K.

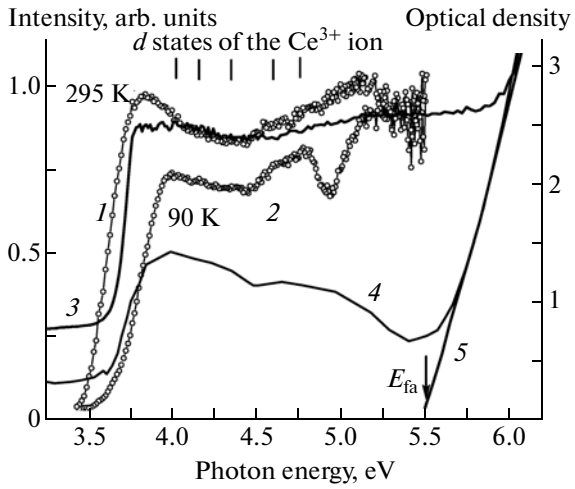

Fig. 3. (*1*, *2*) PL excitation spectra for the emission band at 380 nm, (*3*) absorption spectrum of $LaBr_3$: Ce,Hf (5%), (*4*) absorption spectrum of $LaBr_3$: Ce (0.5%) taken from [14], and (*5*) linear approximation of the fundamental absorption edge. Shown also is the energy position of the *d* states of the Ce^{3+} ion in $LaBr_3$: Ce at T = 10 K according to the experimental data [4] and calculations [7].

also presents the absorption spectrum of $LaBr_3$: Ce (0.5%) with a low concentration of cerium ions, which was converted by us from the transmission spectrum reported in [14]. The optical density in the range of 3.5–5.5 eV depends on the concentration of Ce^{3+} ions and significantly increases at energies above 5.5 eV. A linear approximation of this part of the spectrum allows us to estimate the energy of the onset of the fundamental absorption E_{fa} = 5.5 eV. The PL excitation spectra for bands at 412 and 550 nm are shown in Fig. 4. It can be seen from this figure that there are selective maxima in the transparency region of the crystal at energies of 3.60 and 5.05 eV, respectively.

Figure 5 shows the time-resolved PL excitation spectra of Ce^{3+} centers over a wide energy range spanning the UV, VUV, and XUV ranges. The luminescence efficiency of Ce^{3+} centers sharply decreases at energies above 5.5 eV and smoothly increases at E_{exc} > 13 eV. It should be noted that, at E_{exc} > 70 eV, this spectrum, against the background of the monotonic increase, contains narrow dips and a broad minimum in the region of 120 eV. A detailed analysis of the PL excitation spectrum in the XUV range was made in our previous papers [11, 12]. The PL decay kinetics depends substantially on the excitation energy (Fig. 6). At E_{exc} > 5.5 eV, the PL decay kinetics has slow components in the microsecond range. Figure 7 presents the results of thermal activation spectroscopy: the XL spectra, the temperature dependences of the XL intensity for Ce^{3+} centers and STEs, and the TL curves measured in different recording modes of thermally stimulated luminescence (TSL) for $LaBr_3$: Ce,Hf crystals exposed to X-ray irradiation at T = 90 K.

The gamma-ray source spectrum measured according to the standard technique with a scintillation block consisting of a detector based on $LaBr_3$: Ce,Hf (d = 18 mm, h = 3 mm) and a Hamamatsu R6231 photomultiplier is shown in Fig. 8.

4. DISCUSSION OF THE EXPERIMENTAL RESULTS

The analysis of the presented spectra has demonstrated that, in the $LaBr_3$: Ce,Hf crystals, there are Ce^{3+} centers located in regular sites of the crystal lattice (in what follows, *A* centers), as well as Ce^{3+} centers situated in the vicinity of the defects of the crystal structure (*B* centers). PL of the *B* centers under intracenter excitation has the decay time $\tau = 20 \pm 1$ ns, which is shorter than the PL decay time of the *A* centers (τ = 23 ns). The maxima of the bands in the PL spectrum are shifted toward lower energies, and the Stokes shift remains almost unchanged. A similar pattern is observed in some matrices doped with Ce^{3+} ions and reasonably interpreted as PL of the Ce^{3+} centers located near the defects of the crystal structure (see, for example, [15]). PL of the *B* centers is efficiently excited by photons with an energy of 3.6 eV; however, the $f \longrightarrow d$ electronic transitions in the absorption spectra of Ce^{3+} ions in this energy range do not manifest themselves, which indicates a relatively low concentration of *B* centers. That is why only the *A* centers can be observed in the XL spectra.

It was found that, apart from the *B* centers, the $LaBr_3$: Ce,Hf crystals contain new lattice defects. The PL spectrum at T = 8 K has a broad band with the

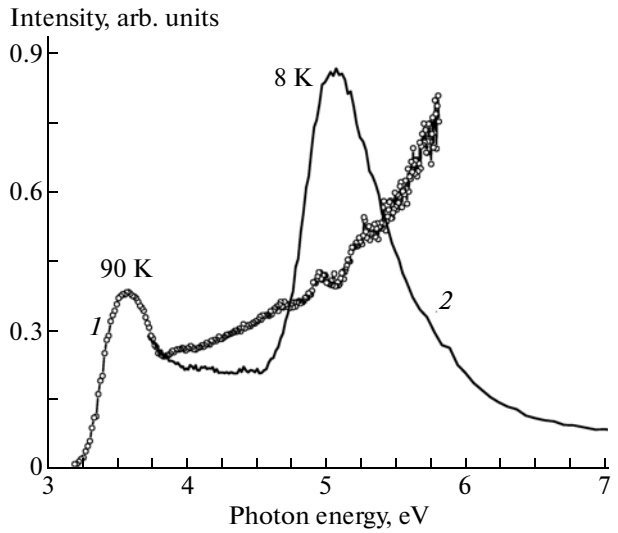

Fig. 4. PL excitation spectra for bands at (*1*) 412 and (*2*) 550 or 600 nm in $LaBr_3$: Ce,Hf.

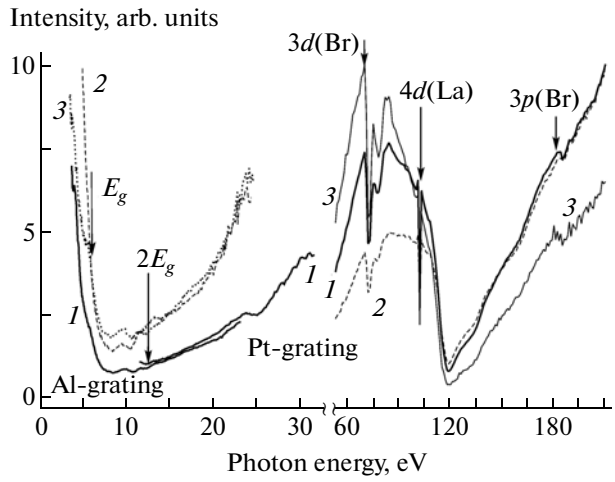

Fig. 5. Time-resolved PL excitation spectra (emission band at 380 nm) of $LaBr_3$: Ce,Hf at $T = 295$ K: (*1*) time-integrated, (*2*) fast, and (*3*) slow components. Spectrum *1* was measured using Al and Pt diffraction gratings.

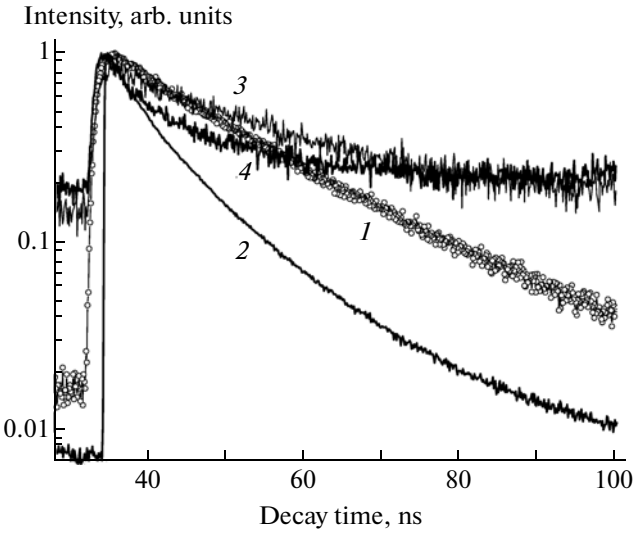

Fig. 6. PL decay kinetics of $LaBr_3$: Ce,Hf (band emission at 380 nm) at excitation energies E_{exc} = (*1*) 3.8–4.6 ($T = 8$ K), (*2*) 5.5–6.4 ($T = 8$ K), (*3*) $E_{exc} = 20.7$ eV ($T = 8$ K), and (*4*) 500 eV ($T = 295$ K).

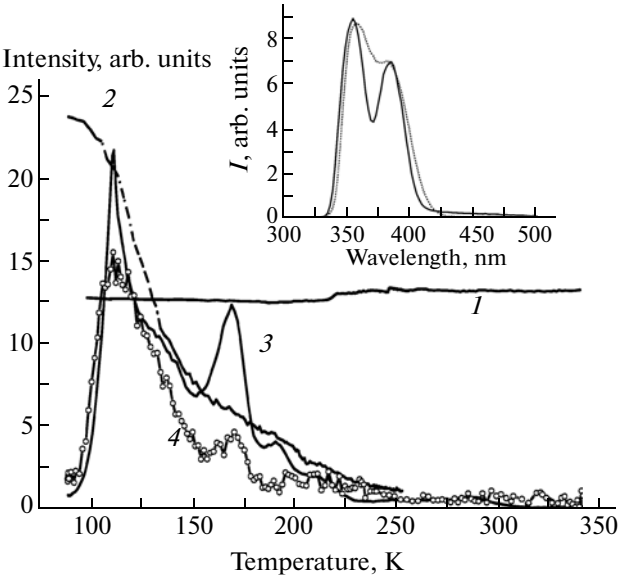

Fig. 7. (*1*, *2*) Temperature dependences of the XL intensity in bands at (*1*) 380 and (*2*) 450 nm. (*3*, *4*) TL curves of the X-ray-irradiated $LaBr_3$: Ce,Hf crystals at $T = 90$ K, measured (*3*) in the wavelength range 300–600 nm and (*4*) in the 356 nm emission band of Ce^{3+} centers. The inset shows the XL spectrum at $T = 90$ (solid line) and 295 K (dotted line).

maximum at 550 nm (2.25 eV, FWHM = 0.8 eV). The PL efficiency has a maximum value at $E_{exc} = 5.05$ eV (the Stokes shift is 2.8 eV) and decreases under excitation in the fundamental absorption edge and interband transitions. On this basis, it can be concluded that we are dealing here with the intracenter PL, and the efficiency of energy transfer by excitons or itinerant charge carriers to this emission center is relatively low. We cannot yet associate this band with the presence of the Hf^{4+} ions as substitutional ions in the crystal and, consequently, with the formation of an impurity–vacancy complex. Furthermore, there are no luminescence manifestations of HfO_2, which has a band in the low-temperature PL spectra in the region of 4.2–4.4 eV and a PL excitation band in the region of 5.8 eV [16]. In this case, the appearance of a similar band should be expected because of the sensitization in the PL excitation spectrum of Ce^{3+} centers. The structure

of this PL center remains unclear and requires further investigation.

The optical density in the energy range of 3.5–5.5 eV depends on the concentration of Ce^{3+} ions. Figure 3 shows the energy position of the *d* states of the Ce^{3+} ion in $LaBr_3$: Ce according to experimental data obtained in [4] and calculations presented in [7]. We note their good correlation with the measured absorption spectrum. The sharp increase and high value of the optical density at energies higher than 5.7 eV indicate the onset of the fundamental absorption. The linear approximation shown in Fig. 3 allows us to estimate the energy of the onset of the fundamental absorption $E_{fa} = 5.5$ eV. In this energy range, the nanosecond PL decay kinetics of Ce^{3+} centers has slow components in the microsecond range (Fig. 5, curve *3*; Fig. 6), which indicates the participation of itinerant charge carriers in the formation of PL. Based on the data presented above, we can estimate the minimum energy of interband transitions in $LaBr_3$: $E_g \sim 6.2$ eV. It should be noted that the values of E_g and E_{fa} differ from the data reported in [5, 12]. However, the presented value agrees very well with the calculations of the band structure of $LaBr_3$, according to which with inclusion of the spin–orbit interaction, we have the energy $E_g =$ 5.99–6.19 eV [17]. Apparently, the use of other experimental techniques, in particular, the measurement of the Urbach tail absorption for $LaBr_3$, will make it possible to obtain the exact value of E_g. The determination of the energy E_g from the reflection spectra of these crystals is hardly possible, because the reflection spectra of rare-earth halide crystals do not exhibit exciton states, which is determined by the *pd* genealogy of the top of the valence band and the conduction band of these crystals [18].

The PL excitation efficiency of Ce^{3+} impurity centers drops in the range of the fundamental absorption edge and interband transitions (Fig. 5). This drop in the PL efficiency is associated with the competition of the capture of itinerant charge carriers by defects of the crystal structure and with the formation of STEs, but it is primarily determined by the nonradiative annihilation of itinerant charge carriers on the crystal surface due to the high value of the absorption coefficient. With increasing excitation energy E_{exc}, an increase in the kinetic energy of itinerant carriers leads to the stabilization of the PL efficiency, and at energies $E_{exc} > 13$ eV, the PL efficiency increases monotonically. Although the absorption spectrum in this energy range is unknown, nonetheless, taking into account the results of investigations of the PL excitation spectra in the XUV region [12] (see the right part of Fig. 5), we assume that, at $E_{exc} > 13$ eV (more than $2E_g$), the effect of multiplication of electronic excitations (MEE) manifests itself, which is an attribute of the effective scintillation process. For $LaBr_3$ crystals, the valence band, according to calculations [17], is

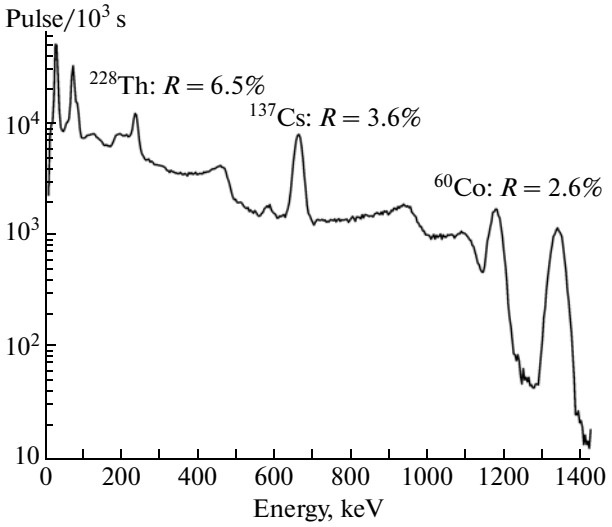

Fig. 8. Spectrum of gamma-ray sources ^{228}Th, ^{137}Cs, and ^{60}Co, measured using a $LaBr_3$: Ce,Hf detector (d = 18 mm, h = 3 mm) and a Hamamatsu R6231 photomultiplier. The discrimination threshold is 20 keV. The energy resolution is given for the main gamma-ray lines.

formed predominantly by the bromine 4*p* states and has a weak dispersion, whereas the total width of the valence band E_v, according to X-ray photoelectron spectroscopy and band structure calculations [17], does not exceed 4 eV. For crystals with a narrow valence band and a large effective mass of holes, the threshold energy of the MEE effect, in accordance with modern concepts of the MEE theory [19], should lie just in the region $(2–3)E_g$. Since $E_v < E_g$ in $LaBr_3$, we can assume that the MEE mechanism is realized by means of the generation of secondary electron–hole pairs due to inelastic scattering of hot photoelectrons.

Let us now turn to the results of thermal activation spectroscopy. As follows from Fig. 7, the XL intensity of the Ce^{3+} centers hardly depends on the temperature in the range of 90–450 K, whereas the STE luminescence is quenched at temperatures above 100 K. This temperature dependence has two stages. The XL quenching activation energy calculated according to the Mott formula in the temperature range of 90–160 K (the first main stage of quenching) is equal to 84 meV. At the same time, the position of the main peak at 114 K on the TL curve corresponds to the thermal quenching region of STE luminescence. The estimation of the activation energy ΔE for the peak at 114 K gives a surprisingly close value: $\Delta E = 86$ meV (calculation was performed according to the Lushchik method for the bimolecular process). The spectral composition of these TSL peaks, as follows from Fig. 7, corresponds to the Ce^{3+} emission. Note that the position and spectral composition of the main peak at 114 K is well consistent with the TSL data presented in [20]: for $LaBr_3$: Ce (5%), the main peak of

the TL curve is in the region of 120 K, and its spectral composition corresponds to the Ce^{3+} emission. Hence, it follows that, first, during heating of the irradiated crystal, the recombination of electrons released from the trapping centers (defects) occurs at cerium centers. Second, since the STE luminescence quenching is not accompanied by an increase in the XL efficiency of impurity centers, the exciton mechanism of the energy transfer STE $\longrightarrow$ Ce^{3+} is not observed and the STE luminescence quenching during heating is associated with the exciton autoionization (formation of itinerant electrons and holes). However, the STE concentration in the studied $LaBr_3$: Ce,Hf crystals with a relatively high concentration of crystal lattice defects is rather low. Therefore, the STE autoionization during heating does not lead to a noticeable increase in the luminescence intensity of the Ce^{3+} centers.

Figure 8 shows the gamma-ray source spectrum measured using a scintillation block specially fabricated for a portable gamma-ray spectrometer and consisting of a detector based on $LaBr_3$: Ce,Hf (d = 18 mm, h = 3 mm) and a Hamamatsu R6231 photomultiplier. The spectrum shows a good energy resolution for the main gamma-ray lines and the characteristic X-ray radiation in the range of 30–90 keV.

5. CONCLUSIONS

This study was carried out using different spectroscopic methods. The main results can be summarized as follows. It was found that, in the studied crystals, there are Ce^{3+} centers located in the vicinity of the defects of the crystal structure. These centers have specific spectral and kinetic characteristics that differ from the parameters of the Ce^{3+} centers located in regular lattice sites. It was also found that the crystals exhibit PL due to new point defects; however, their nature has not yet been determined. Based on the analysis of the absorption and PL excitation spectra, we determined the minimum energy of interband transitions in $LaBr_3$: $E_g \sim 6.2$ eV. This result is well consistent with the band structure calculations [17]. At energies $E_{exc} > 13$ eV (more than $2E_g$), the observed MEE effect is due to the generation of secondary electron–hole pairs as a result of inelastic scattering of hot photoelectrons. The thermal activation studies revealed the main channels of electronic excitation energy transfer to impurity centers.

In general, the PL spectroscopy data showed that, in the $LaBr_3$: Ce,Hf crystals with a low hygroscopicity, the concentration of lattice defects is higher than that in the $LaBr_3$: Ce crystals. However, this does not lead to a significant decrease in the light yield and to a change in the luminescence decay kinetics of Ce^{3+} centers. The presented results demonstrated that these crystals can be successfully used in X-ray and gamma spectrometry.

ACKNOWLEDGMENTS

We would like to thank V.Yu. Ivanov for his support of our work and O.V. Ignat'ev for performing the spectrometric measurements.

This study was supported in part by the Hamburg Synchrotron Radiation Laboratory HASYLAB at DESY (Hamburg, Germany) (project nos. II-20110050 and II-20080119 EC) and the Ministry of Education and Science of the Russian Federation (agreement no. 14.A18.21.0076).

REFERENCES

1. E. V. D. van Loef, P. Dorenbos, C. W. E. van Ejik, K. Kramer, and H. U. Gudel, Appl. Phys. Lett. **79**, 1573 (2001).
2. K. S. Shah, J. Glodo, W. W. Moses, S. E. Derenzo, and M. J. Weber, Nucl. Instrum. Methods Phys. Res., Sect. A **505**, 76 (2003).
3. http://www.detectors.saint-gobain.com/Brillance380.aspx.
4. E. V. D. van Loef, P. Dorenbos, C. W. E. van Eijk, K. W. Krämer, and H. U. Gudel, Phys. Rev. B: Condens. Matter **68**, 045108 (2003).
5. P. Dorenbos, E. V. D. van Loef, A. P. Vink, E. van der Kolk, C. W. E. van Eijk, K. W. Kramer, H. U. Gudel, W. M. Higgins, and K. S. Shah, J. Lumin. **117**, 147 (2006).
6. G. Bizarri and P. Dorenbos, Phys. Rev. B: Condens. Matter **75**, 184302 (2007).
7. J. Andriessen, E. van der Kolk, and P. Dorenbos, Phys. Rev. B: Condens. Matter **76**, 075124 (2007).
8. I. V. Khodyuk and P. Dorenbos, J. Phys.: Condens. Matter **22**, 485402 (2010).
9. K. S. Shah, J. Glodo, M. Klugerman, W. W. Moses, S. E. Derenzo, and M. J. Weber, IEEE Trans. Nucl. Sci. **50**, 2410 (2003).
10. V. A. Pustovarov, V. Yu. Ivanov, D. I. Vyprintsev, and N. G. Shvalev, DESY, HASYLAB Annual Rep. 20111577 (2011).
11. V. A. Pustovarov, V. Yu. Ivanov, D. I. Vyprintsev, and N. G. Shvalev, Tech. Phys. Lett. **38** (9), 784 (2012).
12. V. A. Pustovarov, A. N. Razumov, V. Yu. Ivanov, D. I. Vyprintsev, and N. G. Shvalev, Bull. Russ. Acad. Sci.: Phys. **77** (2), 217 (2013).
13. D. I. Vyprintsev, RF Patent 2426694 (February 15, 2010).
14. H. Chen, C. Zhou, P. Yang, and J. Wan, J. Mater. Sci. Technol. **25** (6), 753 (2009).
15. S. I. Omelkov, M. G. Brik, M. Kirm, V. A. Pustovarov, V. Kiisk, I. Sildos, S. Lange, S. I. Lobanov, and L. I. Isaenko, J. Phys.: Condens. Matter **23**, 10550 (2011).
16. M. Kirm, J. Aarik, M. Jürgens, and I. Sildos, Nucl. Instrum. Methods Phys. Res., Sect. A **537**, 251 (2005).
17. D. Åberg, B. Sadigh, and P. Erhart, Phys. Rev. B: Condens. Matter **85**, 125134 (2012).
18. G. G. Olson, D. W. Lynch, and M. Piacentini, Phys. Rev. B: Condens. Matter **18** (10), 5740 (1978).
19. A. Lushchik, E. Feldbach, R. Kink, Ch. Lushchik, M. Kirm, and I. Martinson, Phys. Rev. B: Condens. Matter **53** (9), 5379 (1996).
20. O. Sellès, M. Fasoli, A. Vedda, M. Martini, and D. Gourier, Phys. Status Solidi C **4** (3), 1004 (2007).

Translated by O. Borovik-Romanova